

the nearer range, the better spatial resolution could be obtained. So the side-scattering lidar is very suitable to detect aerosol spatial distribution in the boundary layer from the surface.

In this paper, the aerosol extinction coefficient profile is retrieved by our self-developed CCD side-scattering lidar, and $PM_{2.5}$ mass concentration is measured simultaneously in ground level by a particle matter monitor. Syncretizing these two datasets measured at same time and same place, the profile of $PM_{2.5}$ mass concentration can be derived in the boundary layer. In Sect. 2, the instrumentation is introduced; and the methodology for extinction and $PM_{2.5}$ profiles is shown in Sect. 3; then the results is discussed in Sect. 4; followed by the summary and conclusion in the last Sect. 5.

2 Instruments

The measurement system is consisted of a CCD side-scattering lidar and a $PM_{2.5}$ mass monitor as shown in Fig. 1. The subsystem of side-scattering lidar consists of laser, CCD camera, geometric calibration, data acquisition and control computer. The light source is a Nd:YAG laser (Quantel Brilliant) emitting laser pulses in 20 Hz at 532 nm wavelength. The side-scattering light is received by a CCD camera with 3352×2532 pixels. The exposed time is set 5 min according to the signal-to-noise ratio with a maximum relative error of 1.5 % caused by noises (Ma et al., 2014), and there is an interference filter with 30 nm bandwidth in front of CCD lens. Using geometric calibration, the relationship between the pixels and corresponding to the scattering lights in laser beam is determined. The computer acquires the CCD camera data and controls timing sequence between laser and CCD camera. $PM_{2.5}$ mass monitor works simultaneously, and the output product is the average $PM_{2.5}$ mass concentration through one hour. In Fig. 1, z is the detecting distance, D is the distance from CCD camera to laser beam, θ is the scattering angle, $d\theta$ is the FOV of one pixel. The detailed specifications of the CCD side-scattering lidar (C-lidar) are described in the previous work (Tao et al., 2014a) and shown in Table 1.

Profiling the $PM_{2.5}$ mass concentration vertical distribution in the boundary layer

Z. Tao et al.

Title Page

Abstract

Introduction

Conclusions

References

Tables

Figures



Back

Close

Full Screen / Esc

Printer-friendly Version

Interactive Discussion



The PM_{2.5} mass monitor, named Thermo Scientific TEOM 1405 Ambient Particulate Monitor, can carry out continuous measurement of ambient particulate concentrations with the resolution of 0.1 µg m⁻³ and the precision of ±2.0 µg m⁻³ (one hour averaged).

3 Methodology

3.1 Retrieved method of aerosol extinction profile

The side-scattering lidar equation is expressed as (Tao et al., 2014b):

$$P(z, \theta) = \frac{P_0 K A}{D} \left(\frac{\beta_1(z, \pi)}{f_1(\pi)} f_1(\theta) + \frac{\beta_2(z, \pi)}{f_2(\pi)} f_2(\theta) \right) \cdot \exp \left(-\tau - \frac{\tau}{\cos(\pi - \theta)} \right) d\theta \quad (1)$$

Where $P(z, \theta)$ is the received power at height z and scattering angle θ by a pixel, P_0 is laser pulse energy, K is a system constant including the optical and electronic efficiency and A is the area of CCD camera lens, $\beta(z, \pi)$ is backscattering coefficient, $f(\theta)$ is phase function. Subscripts “1” and “2” represent aerosol and molecule scattering, respectively. τ is optical depth, $\alpha(z)$ is extinction coefficient, and $\tau = \int_0^z (\alpha_1(z') + \alpha_2(z')) dz'$.

In general, for Eq. (1), there is six unknown variables, i.e. phase function, backscattering and extinction coefficients of aerosol and molecule. Three unknown variables for molecule are calculated from standard molecular model using Rayleigh scatter theory. A prior assumption has to be given, i.e. lidar ratio (extinction-to-backscattering ratio) of aerosol, in order to reduce an unknown. The value of 50 sr is used as lidar ratio at 532 nm wavelength in our algorithm. The aerosol phase function is determined from a sky-radiometer (for example, a Prede POM-02 sky-radiometer made in Japan). Then only one variable (the backscattering or extinction coefficient of aerosol) is left, which can be retrieved from Eq. (1) as following.

In our experiment, vertical-pointing backscattering lidar (V-lidar) and C-lidar worked simultaneously. For V-lidar data processing, it is a traditional way to select the clear point about the tropopause as reference point where assumed has minimum aerosol.

Profiling the PM_{2.5} mass concentration vertical distribution in the boundary layer

Z. Tao et al.

Title Page

Abstract

Introduction

Conclusions

References

Tables

Figures



Back

Close

Full Screen / Esc

Printer-friendly Version

Interactive Discussion



increases to three sub-peaks of 29, 33, and $33 \mu\text{g m}^{-3}$ in the floating layer, respectively. The vertical distribution of $\text{PM}_{2.5}$ at 21:30 BT measured in Hefei site on September 21 2014 depicts a rich structures.

4.2 Case II: pollutant night

On 17 March 2014, it was also clear at night, with the south wind of not more than 3 m s^{-1} near the earth surface. The temperature varies from 18.2 to 21.7°C with a decreasing trend and the RH increases from 58 to 70 % during the time span of 19:30–24:00 BT as shown in Fig. 4a. The distance D between laser beam and CCD camera is 23.90 m.

Figure 4b plots the hourly mean value of K varying around $0.011 \text{ km}^{-1}/(\mu\text{g m}^{-3})$ with the minimum 0.009 and the maximum 0.012, which also indicates an approximate constant value during this experimental case. Then $\text{PM}_{2.5}$ profile is given accordingly by using the specific coefficient K and the aerosol extinction coefficient profile. The spatio-temporal distribution of $\text{PM}_{2.5}$ mass concentration for this case in Hefei site is shown in Fig. 4c. The $\text{PM}_{2.5}$ is almost enclosed below 1.8 km a.g.l. with a maximums value $70 \mu\text{g m}^{-3}$, indicating a light pollutant night in Hefei. Between 0.6 and 1.8 km a.g.l., the $\text{PM}_{2.5}$ value is almost constant indicating a well mixed layer. The maximum value of $\text{PM}_{2.5}$ lies near the earth surface layer and forms a rather stable aerosol structure, which will cause a haze day with poor visibility.

It is remarked from Fig. 4d that the $\text{PM}_{2.5}$ value remains $20 \mu\text{g m}^{-3}$ at 0.9–1.8 km a.g.l., and increases to $30 \mu\text{g m}^{-3}$ at 0.3 km a.g.l., then increases rapidly to a peak of $55 \mu\text{g m}^{-3}$ at the earth surface. The vertical distribution of $\text{PM}_{2.5}$ at 21:30 BT measured in Hefei site on 17 March 2014 depicts a stable structure.

4.3 Case III: heavy pollutant night

On 13–14 February 2015, it was also cloud-free at night, with the northwest wind of not more than 3 m s^{-1} near the ground. The temperature varies from 10.7 to 9.1°C with

Profiling the $\text{PM}_{2.5}$ mass concentration vertical distribution in the boundary layer

Z. Tao et al.

Title Page

Abstract

Introduction

Conclusions

References

Tables

Figures



Back

Close

Full Screen / Esc

Printer-friendly Version

Interactive Discussion



Profiling the PM_{2.5} mass concentration vertical distribution in the boundary layer

Z. Tao et al.

Title Page

Abstract

Introduction

Conclusions

References

Tables

Figures



Back

Close

Full Screen / Esc

Printer-friendly Version

Interactive Discussion



a decreasing trend and the RH increases speedily from 31 to 68 % during the time span of 18:30–02:00 BT, then keeps around 65 % in the late period of 02:00–05:30 BT as shown in Fig. 5a. The distance D between laser beam and CCD camera is 19.40 m.

Figure 5b plots the hourly mean value of K varying from 0.006 to 0.007 km⁻¹ (μg m⁻³)⁻¹, which also indicates an approximate constant value during this experimental case. But this value is quite different from that obtained from CASE I and CASE II maybe due to the differences of aerosol size distribution and refractive index. The PM_{2.5} profile is calculated accordingly by using the K value and the aerosol extinction coefficient profile. At the meanwhile, the spatio-temporal distribution of PM_{2.5} mass concentration for this case in Hefei site is shown in Fig. 5c. The PM_{2.5} is lifted up to 2.1 km a.g.l. with a maximum value 210 μg m⁻³, indicating a heavy pollutant night in Hefei. During the observation period, there are three distinct layers (i.e., the floating layer, the clean layer, and the earth surface layer) with a gradual fall in height from the evening to the next morning. The typical height for the floating layer decreases from 1.2–1.8 km a.g.l. to 0.5–1.0 km a.g.l. and the peak value of PM_{2.5} for this layer is about 150 μg m⁻³. The PM_{2.5} value for the fair layer in middle part varies from 30 to 50 μg m⁻³. The top height of the earth surface layer decreases from 0.9 km a.g.l. at 18:00 BT to 0.3 km a.g.l. at 06:00 BT, which leads to a more stable structure. The maximum value of PM_{2.5} lies near the earth surface layer, especially below 0.3 km a.g.l., where a high value region of PM_{2.5} (i.e., 200 μg m⁻³) exists all along from 20:00 to 04:00 BT, which will cause a heavy haze day with worse visibility.

It is remarked from Fig. 5d that the PM_{2.5} value takes on a sub-peak of 110 μg m⁻³ at 1.2 km a.g.l., and increases rapidly from 20 μg m⁻³ at 0.8 km a.g.l. to another sub-peak of 190 μg m⁻³ at 0.4 km a.g.l., then increases rapidly again to a peak of 210 μg m⁻³ at the earth surface. The vertical distribution of PM_{2.5} at 21:00 BT measured in Hefei site on February 13–14, 2015 appears a more stable and rich structure.

5 Summary and conclusion

A new measurement technology of $PM_{2.5}$ mass concentration profile in near-ground is present in this paper based on a CCD side-scatter lidar and a $PM_{2.5}$ detector. Our new method is proved to be effective through three cases measured during nighttime in SKYNET Hefei site. And some useful conclusions are summarized as following:

1. Five types of aerosol from OPAC, prevail in Hefei site, are used to testify their extinction property depending on RH, only to find that there is rarely reliant on RH when RH is less than 70 %.
2. The specific coefficient K , which is related to aerosol size distribution, refractive index, and atmospheric relative humidity, may contain a fix value under the suitable condition when RH is less than 70 %, though it may not be the same for each case. So, the $PM_{2.5}$ mass concentration profile can be easily derived from vertical distribution of extinction coefficient for aerosol.
3. The $PM_{2.5}$ is always loading in the planet boundary layer with a multi-layers structure, indicating its complexity of the vertical distribution. And there is a higher lifting height under the heavy polluted weather condition, demonstrating air pollution may break through near the surface into a higher altitude and join in further transportation.
4. The high value of $PM_{2.5}$ remains near the ground and forms a stable structure, especially in haze day, which will cause a bad weather condition, such as low visibility.
5. Our new method for $PM_{2.5}$ mass concentration profile is a useful approach for improving our understanding of air quality, and atmospheric environment, which can also provide critical information for daily air quality forecast. Further investigation will be carried on in the near future when RH is larger than 70 % including the potential variation of specific coefficient K .

Profiling the $PM_{2.5}$ mass concentration vertical distribution in the boundary layer

Z. Tao et al.

Title Page

Abstract

Introduction

Conclusions

References

Tables

Figures



Back

Close

Full Screen / Esc

Printer-friendly Version

Interactive Discussion



Acknowledgements. This research is supported by the National Natural Science Foundation of China (Nos. 41175021 and 41305022), the Ministry of Science and Technology of China (No. 2013CB955802), and the Anhui Provincial Natural Science Foundation (No. 1308085MD53). We would also like to thank all anonymous reviewers for their constructive and insightful comments.

References

- An, J., Zhang, R., and Han, Z.: Seasonal changes of total suspended particles in the air of 15 big cities in northern parts of China, *Climatic and Environ. Res.*, 5, 25–29, 2000.
- Bernes, J. E., Bronner, S., and Becket, R.: Boundary layer scattering measurements with a charge-coupled device camera lidar, *Appl. Optics*, 42, 2647–2652, 2003.
- Bo, G., Liu, D., and Wu, D.: Two-wavelength lidar for observation of aerosol optical and hygroscopic properties in fog and haze days, *Chinese Journal of Lasers*, 41, 0113001, doi:10.3788/cjl201441.0113001, 2014.
- Cordero, L., Wu, Y., Gross, B. M., and Moshary, F.: Use of passive and active ground and satellite remote sensing to monitor fine particulate pollutants on regional scales, *Proc. SPIE 8366, Advanced Environmental, Chemical, and Biological Sensing Technologies IX*, 83660M, doi:10.1117/12.918765, 2012.
- He, X., Deng, Z., Li, C., Lau, A. K., Wang, M., Liu, X., and Mao, J.: Application of MIDIS AOD in surface PM₁₀ evaluation, *Acta Scientiarum Naturalium Universitatis Pekinensis*, 46, 178–184, 2010.
- Hess, M., Koepke, P., and Schult, I.: Optical properties of aerosols and clouds: the software package OPAC, *B. Am. Meteorol. Soc.*, 79, 831–844, 1998.
- Li, Q., Li, C., Wang, Y., Lin, C., Yang, D., and Li, Y.: Retrieval on mass concentration of urban surface suspended particulate matter with lidar and satellite remote sensing, *Acta Scientiarum Naturalium Universitatis Pekinensis*, 49, 673–682, 2013.
- Ma, X., Tao, Z., Ma, M.: The retrieval of side-scatter lidar signal based on CCD technique, *Acta Optica Sinica*, 34, 0201001, doi:10.3788/aos201434.0201001, 2014.
- Mao, F., Gong, W., and Li, J.: Geometrical form factor calculation using Monte Carlo integration for lidar, *Opt. Laser Technol.*, 44, 907–912, 2012.

Profiling the PM_{2.5} mass concentration vertical distribution in the boundary layer

Z. Tao et al.

Title Page

Abstract

Introduction

Conclusions

References

Tables

Figures



Back

Close

Full Screen / Esc

Printer-friendly Version

Interactive Discussion



Profiling the PM_{2.5} mass concentration vertical distribution in the boundary layer

Z. Tao et al.

Title Page

Abstract

Introduction

Conclusions

References

Tables

Figures



Back

Close

Full Screen / Esc

Printer-friendly Version

Interactive Discussion



- Mao, J., Zhang, J., and Wang, M.: Summary comment on research of atmospheric aerosol in China, *Acta Meteorol. Sin.*, 60, 625–634, 2002.
- Pesch, M. and Oderbolz, D.: Calibrating a ground based backscatter lidar for continuous measurements of PM_{2.5}, lidar technology, techniques, and measurements for atmospheric remote sensing III, *Proc. Of SPIE* 6750, 67500K, doi:10.1117/12.737732, 2007.
- Sano, I., Mukai, M., Okada, Y., Mukai, S., Sugimoto, N., Matsui, I., and Shimizu, A.: Improvement of PM_{2.5} analysis by using AOT and lidar data remote sensing of the atmospheric and clouds II, *Proc. Of SPIE* 7152, 71520M, doi:10.1117/12.804903, 2008.
- Tao, Z., Liu, D., and Ma, X.: Development and case study of side-scatter lidar system based on charge-coupled device, *Infrared and Laser Engineering*, 43, 3282–3286, 2014a.
- Tao, Z., Liu, D., Wang, Z., Ma, X., Zhang, Q., Xie, C., Bo, G., Hu, S., and Wang, Y.: Measurements of aerosol phase function and vertical backscattering coefficient using a charge-coupled device side-scatter lidar, *Opt. Express*, 22, 1127–1134, 2014b.
- Tao, Z., Liu, D., Ma, X., Shi, B., Shan, H., and Zhao, M.: Vertical distribution of near-ground aerosol backscattering coefficient measured by a ccd side-scattering lidar, *Appl. Phys. B-Lasers O.*, 120, 631–635, 2015.
- Wang, Z., Liu, D., Wang, Z., Wang, Y., Khatri, P., Zhou, J., Takamura, T., and Shi, G.: Seasonal characteristics of aerosol optical properties at the SKYNET Hefei site (31.90° N, 117.17° E) from 2007 to 2013, *J. Geophys. Res.-Atmos.*, 119, 6128–6139, doi:10.1002/2014JD021500, 2014a.
- Wang, Z., Liu, D., and Cheng, Z.: Pattern recognition model for haze identification with atmospheric backscatter lidars, *Chinese Journal of Lasers*, 41, 1113001, doi:10.3788/cjl201441.1113001, 2014b.
- Wang, Z., Liu, D., Wang, Y., Wang, Z., and Shi, G.: Diurnal aerosol variations do affect daily averaged radiative forcing under heavy aerosol loading observed in Hefei, China, *Atmos. Meas. Tech.*, 8, 2901–2907, doi:10.5194/amt-8-2901-2015, 2015a.
- Wang, Z., Tao, Z., Liu, D., Wu, D., Xie, C., and Wang, Y.: New experimental method for lidar overlap factor using a CCD side-scatter technique, *Opt. Lett.*, 40, 1749–1752, 2015b.
- Weitkamp, C.: *Lidar: Range-Resolved Optical Remote Sensing of the Atmosphere*, Springer, New York, 2005.
- Winker, D. H., Hunt, W. H., and McGill, M. J.: Initial performance of assessment of CALIOP, *Geophys. Res. Lett.*, 34, 228–262, 2007.

Profiling the PM_{2.5} mass concentration vertical distribution in the boundary layer

Z. Tao et al.

Title Page

Abstract

Introduction

Conclusions

References

Tables

Figures



Back

Close

Full Screen / Esc

Printer-friendly Version

Interactive Discussion

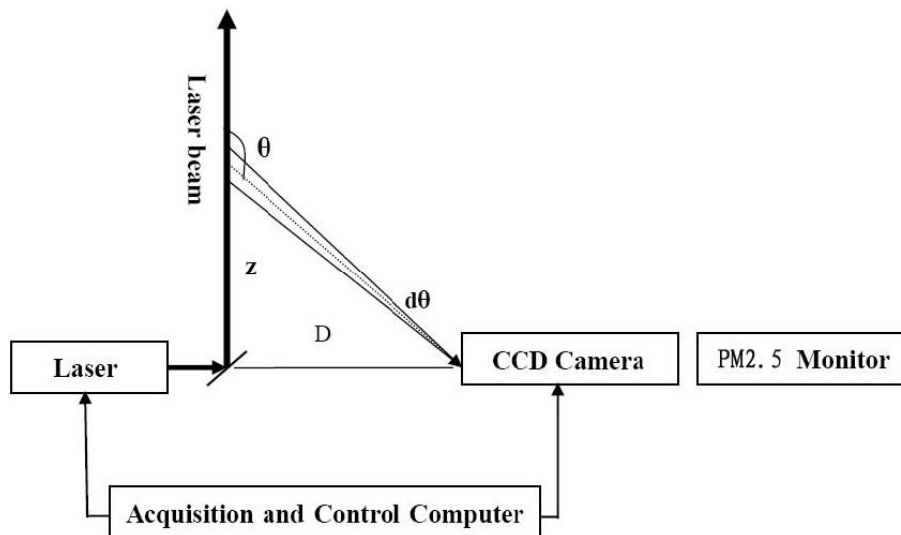


Table 1. The specifications of the C-lidar system.

Laser	(Quantel Brilliant) Nd:YAG
Wavelength (nm)	532
Pulse energy (mJ)	200
Repetition rate (Hz)	20
Detector	(SBIG) ST-8300M
Pixel array	3352 × 2532
Pixel size (μm)	5.4 × 5.4
A/D converter (bits)	16
Wide-angle lens	Walmexpro f/2.8
Lens focal length (mm)	14
CCD sensor	Kodak KAF-8300
Quantum efficiency (532 nm)	~ 55 %
Interference Filter	(Semrock corporation)
Bandwidth (nm)	25.6
Peak transmittance	~ 95 %

Profiling the PM_{2.5} mass concentration vertical distribution in the boundary layer

Z. Tao et al.

**Figure 1.** The diagram of the measurement system.[Title Page](#)[Abstract](#)[Introduction](#)[Conclusions](#)[References](#)[Tables](#)[Figures](#)[◀](#)[▶](#)[◀](#)[▶](#)[Back](#)[Close](#)[Full Screen / Esc](#)[Printer-friendly Version](#)[Interactive Discussion](#)

Profiling the PM_{2.5} mass concentration vertical distribution in the boundary layer

Z. Tao et al.

Title Page

Abstract

Introduction

Conclusions

References

Tables

Figures

◀

▶

◀

▶

Back

Close

Full Screen / Esc

Printer-friendly Version

Interactive Discussion

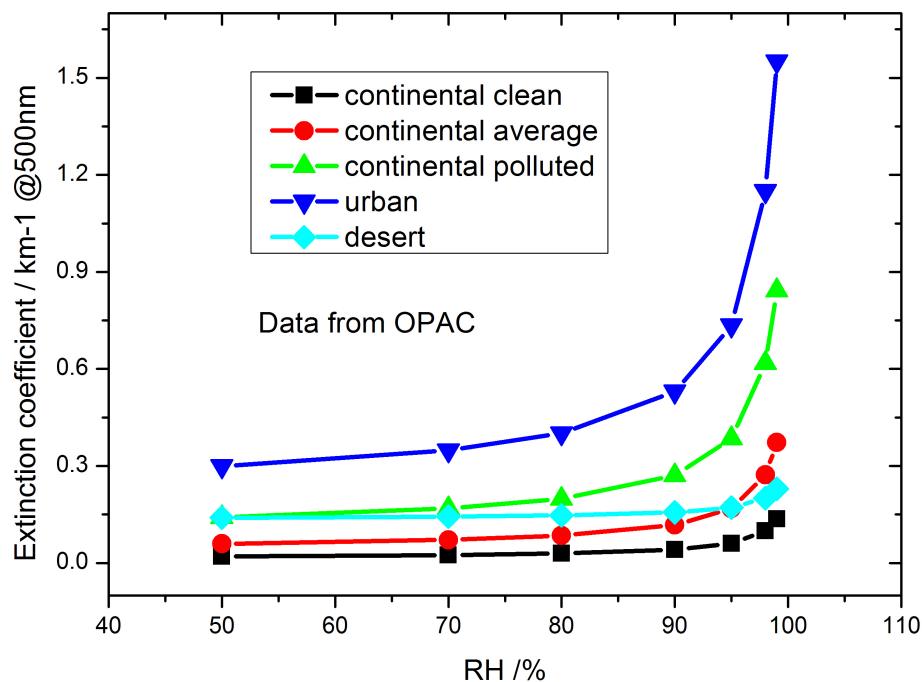


Figure 2. The relationship between aerosol extinction coefficient and atmospheric relative humidity (RH) for five types of aerosol.

Profiling the PM_{2.5} mass concentration vertical distribution in the boundary layer

Z. Tao et al.

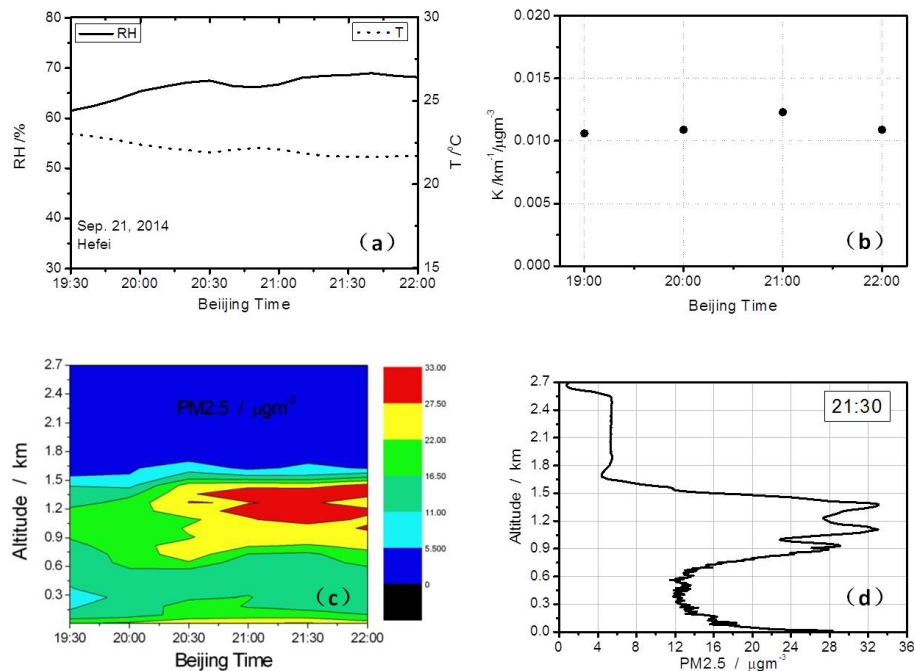


Figure 3. (a) RH and T parameters with time, (b) K value for each hour, (c) time series of PM_{2.5} profile, and (d) vertical distribution of PM_{2.5} at 21:30 BT measured in Hefei site on 21 September 2014.

Profiling the PM_{2.5} mass concentration vertical distribution in the boundary layer

Z. Tao et al.

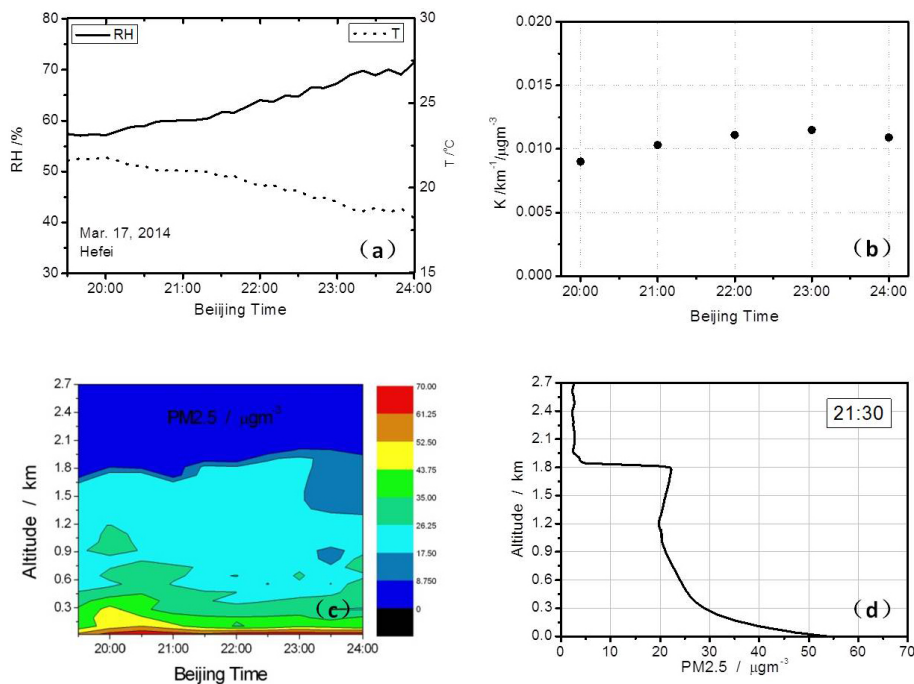


Figure 4. (a) RH and T parameters with time, (b) K value for each hour, (c) time series of PM_{2.5} profile, and (d) vertical distribution of PM_{2.5} at 21:30 BT measured in Hefei site on 17 March 2014.

Profiling the PM_{2.5} mass concentration vertical distribution in the boundary layer

Z. Tao et al.

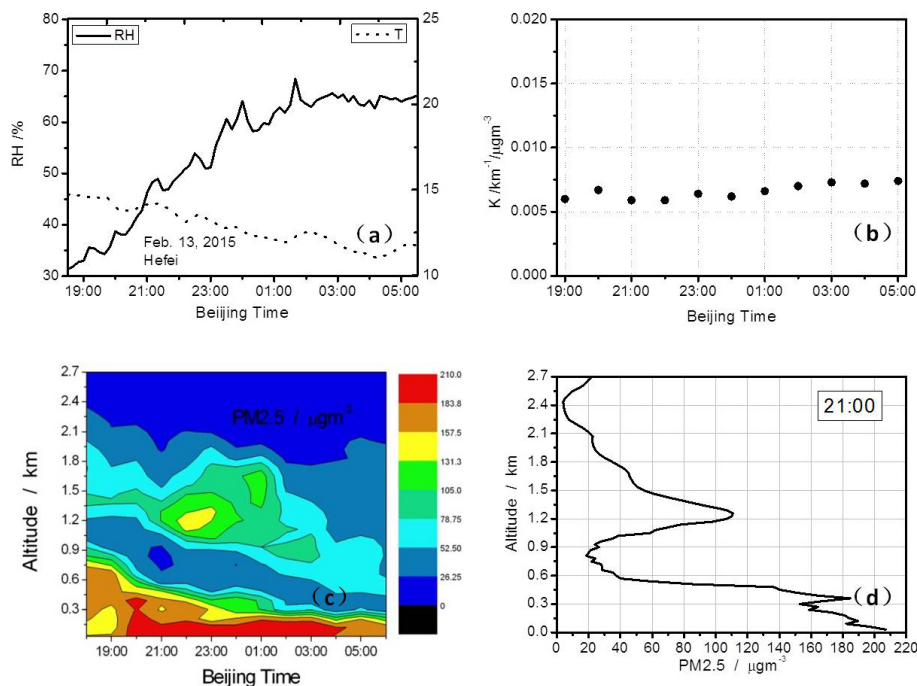


Figure 5. (a) RH and T parameters with time, (b) K value for each hour, (c) time series of PM_{2.5} profile, and (d) vertical distribution of PM_{2.5} at 21:00 BT measured in Hefei site on 13–14 February 2015.